Reservoir Operation under Climate Change Using a Guided Adaptive Search based Particle Swarm Optimization Algorithm

Farshad Rezaei[1], Mehrdad Moghadas[2*]
1- Postdoctoral Research Fellow, Isfahan University of Technology, Isfahan, Iran, Email: farshad.rezaei@gmail.com
2- PhD in Water Structures Engineering, Tehran University. Expert of Isfahan Regional Water Organization, Isfahan, Iran, Email: m.moghadas@ut.ac.ir

Abstract

Human modifications of the landscape along with the increase of the greenhouse gases are all assumed as the factors involved in the climate change. These factors could be affecting the spatial and seasonal precipitation and also could contribute to increase the water demands. These changes in the climatic parameters have resulted in de-naturalizing over half of the world's large river basins. The resulting manipulated stream flows can, in turn, be the main indicators of the water availabilityand also the regulators of the diversity of the ecosystem. Hence, this paper applies two main climate change scenarios (A2 and B1), to optimal operationof the Zayandehroud reservoir, located in west central Iran. A newly proposed Guided Adaptive Search based Particle Swarm Optimization (GuASPSO) algorithm is utilized to solve the optimization problem of this paper. The results suggest the maximum potential of the mentioned reservoir to resist the climate change effects and manage the downstream demands to be maximally met, while the reservoir storage is held at a desirable amount in order to guarantee the sustainability of the surface water during the planning period under the severe climate change conditions.

Keywords: Reservoir operation, Climate change, Particle Swarm Optimization (PSO), Water resources management, Sustainability.

1. INTRODUCTION

Climate changes are part of the hydrologic cycle and cause alterations of natural streamflow regimes. Some of human activities such as dam constructions, land cover changes and water diversions are thought to obscure climate signals in hydrologic systems [1].

Streamflow volume and seasonal variability are of the key indicators of agricultural and urban water availability as well as primary regulators of the distribution and diversity of taxa in fresh water ecosystems [2]. As streamflowis generated by precipitation and snowmelt that is not lost to evapotranspiration or ground water recharge, much of the interannual variability in streamflow can be traced to concurrent variability in climate [3]. As concentrations of greenhouse gases continue to increase, spatial and seasonal precipitation patterns are altered, the proportion of precipitation falling as snow is reduced and evaporative demand is increased [4]. In natural watersheds these changes can directly affect the timing and volume of streamflow. Due to human modifications of the landscape, however, many stream flow regimes throughout the world, including over one half of the world's large river systems, can no longer be considered natural [5]. Primary human modifications include reservoirconstruction and irrigation projects, which, in some cases, canmask, dampen, or even change the sign of natural streamflowtrends.

In the Fourth Annual Intergovernmental Panel Assessment Report, the four main scenarios of A1, B1, A2, and B2 (SRES scenarios) are modeled with five subcategories for each one. The models have been calibrated based on the climatic background and the frequency of observational trends and their performance has been consistently proven over the past 5 years by using atmospheric coupled general climate models.In the below each scenario has been explained:

A1: This scenario depicts a rapidly expanding world with strong interactions and convergences between regions where the per capita income of individuals is more uniform. The world's population will peak in year 5, and then decline, and new and more efficient technologies will be introduced. Three different subdivisions for Group A1 are assumed based on the technology used in the 5th century: A1F1 fossil fuel intensification - A1T non-fossil fuel consumption and A1B fossil and non-fossil fuel consumption.

A2: This scenario depicts a different world in which the population of some areas is reinforced by the emphasis on family values and family traditions, and as a result will grow more than that in the A1 scenario. Per capita economic growth and technology advances are slow.

B1: Population status in B1 is similar to A1 except that the emphasis in this scenario is more on clean energy and the environment. In this scenario, there is a strong emphasis on global solutions for environmental, economic and social sustainability and the pursuit of greater equality between communities.

B2: In B2 scenario, the emphasis is on continued population growth and regional solutions for economic, social and environmental sustainability. Population growth rate in this scenario is lower than that in the scenario A2 and technology growth rate is lower than A2 and B1.

Some past researches using a variety of metrics has demonstrated thatstreamflow trends in natural watersheds closely follow regionalchanges in precipitation and evapotranspiration [6,7] Whilesome researches [4]highlight the influence of climate changes onstreamflow trends, they do not investigate trends in human-modified watersheds, which are more common throughoutthe world.In this research the effect of climate change under two scenarios of A2 and B1 on the Zayandehroud dam management is investigated.

2. STUDY AREA

The Zayandehroudriver is the most important river in central Iran which stretches over a length of 400 km, originating from the Zardkuh mountain and ending in the Gavkhuni swamp after passing through the city of Isfahan. During the last 60 years, the population in the catchment has grown from less than a million to more than 4 million. Today more than one million people live from the land producing wheat, barley and others staple food. Important steel, oil and cement industries have settled along the river which along with numerous smaller enterprises employ more than 300,000 people. The steady growth of region, coupled with the onset of climate change, have taken their respective tolls, leading to increasing water management challenges. While water demand rises, the Zayandehroud's water resources decrease and simultaneously the livelihood of people and important ecosystem dwindle. Temperatures have been rising constantly, while annual rainfall has been declining. Up to a few years ago, the river dominated the cityscape of Isfahan. Its historical bridges and little canals were famous tourist attractive constructions for young and old alike. Numerous species of birds migrate there for the winter in the region around the Gavkhuni Salt Lake and even ventured in the city center. For flamingos the salty lake was an ideal habitat. As the gap between water availability and water demand grows,the different water users increasingly compete for the scarce resource [8]. Then it's important to know how climate change will affect the Zayandehroud dam storage in future and how the scarce should be mitigated.Table 1 presents some main figures related toZayandehroud catchment.

Table 1- Properties of Zayandehroud Catchment (Statistical period: 1971-2013) [8]

Total area	26917 km^2
Share of total area located in Isfahan province	92.9 %
Share of total area located in Chaharmahalvabakhtiari province	7.1%
Average Perticipation	265 mm/year
Average inflow into Zayandehroud dam (include transfers tunnels)	1402 million m^3/year

The Zayandehroud river flow regime not only depends on climatic conditions but also relies on the water releases through the Zayandehroud dam as well as irrigation, domestic and industrial needs.Fig 1 shows the Zayandehroud Basin with water extraction points and irrigation areas in this basin.

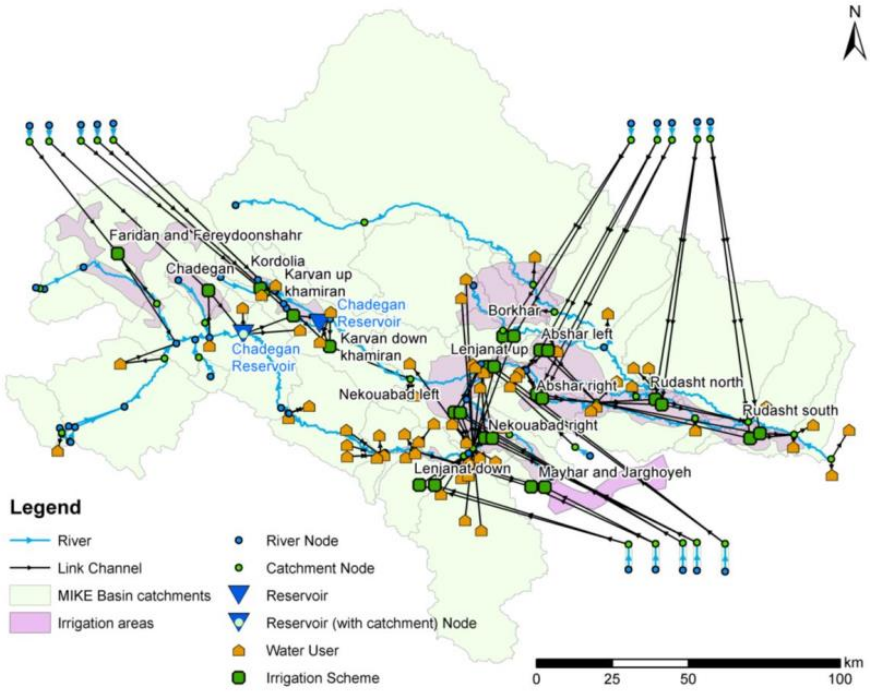

Figure 1.Zayandehroud Basin's Schematic [8]

3. METHODOLOGY

The GuASPSO algorithm [10]is a newly proposed variant of the particle swarm optimization (PSO) algorithm. First, let us depict the formal form of an optimization problem solved by the original PSO algorithm. For a *D*-dimensional optimization problem, it is taken that $X_i = (x_{i1}, x_{i2}, \dots, x_{iD})$ and $V_i = (v_{i1}, v_{i2}, \dots, v_{iD})$are respectively the i^{th} particle's position vector and the velocity vector. If $Pbest_i^t = (p_{i1}, p_{i2}, \dots, p_{iD})$ is the personal best (*Pbest*) position of the i^{th} particle and $Gbest^t = (p_{g1}, p_{g2}, \dots, p_{gD})$represents the global best (*Gbest*) position of the swarm, the velocity and position of each particle in PSO algorithm is updated using Eqs.(1) and (2) [10].

$$V_i^{t+1} = wV_i^t + c_1 r_1 (Pbest_i^t - X_i^t) + c_2 r_2 (Gbest^t - X_i^t) \quad (1)$$

$$X_i^{t+1} = X_i^t + V_i^{t+1} \quad (2)$$

where $i \in \{1, 2, \dots, N\}$; N is the swarm sizeand D is the number of dimensions; superscript t is the iteration number; w is the inertia weight; r_1 and r_2 are two random vectors, and c_1 and c_2 are cognitive and social scaling parameters, respectively. An efficient form of Eq. (1) is the constriction coefficient model shown below

$$V_i^{t+1} = \chi \left[V_i^t + \varphi_1 (Pbest_i^t - X_i^t) + \varphi_2 (Gbest^t - X_i^t)\right] \quad (3)$$

$$\chi = \frac{2k}{|2-\varphi-\sqrt{\varphi(\varphi-4)}|};\ \varphi = \varphi_1 + \varphi_2;\ \varphi_1 = c_1 r_1;\ \varphi_2 = c_2 r_2 \quad (4)$$

whereχ is the constriction factor. The parameter $k \in [0,1]$ in Eq. (4) controls the exploration and exploitation abilities of the swarm, which can be calculated as follows:

$$k = k_{max} - \frac{k_{max} - k_{min}}{t_{max}} \times t \quad (5)$$

wherek_{max} and k_{min} are constants that must be set properly; t is the number of iterations; and t_{max} is the maximum number of iterations.

In PSO, the *Pbests* help the exploration process be done in the search space and the *Gbest* leads the particles to the high-fitness areas in the search space to accomplish exploitation. The GuASPSO algorithm attempts to change the conventional mechanism existing in the original PSO algorithm, mainly in order to better preserve diversity among the solutions generated in the swarm. The proposed mechanism in this algorithm can maintain the diversity at the early stages of the optimization process where the particles need to be dispersed in

all over the search space to facilitate the exploration phase. The algorithm, then, make a well-controlled and well-balanced transition from the exploration to the exploitation by de-emphasizing the diversity and emphasizing the fitness of the promising regions found in the exploration process to guide the particles in the search space. Thus, the GuASPSO may be advantageous to solve the uni-modal functions via diversifying the particles and preventing them from being merged at the initial iterations. The GuASPSO is also a powerful algorithm to handle multi-modal problems by intensifying the convergence to the high-fitness areas and avoiding local optima. Hence, GuASPSO can hold a nice balance between exploration and exploitation capabilities of the PSO algorithm to handle any type of the optimization problems.In this algorithm, a unique *Gbest* particle is assigned to each particle. In this way, the *Gbest* particle is neither so far from, nor so near to its relevant particle, meaning that it is neither involved in a drift leading to lose diversity in the search space, nor is going to be trapped in local optima. However, the drift occurrence is the more important problem the original PSO algorithm is engaged with, especially in the early iterations in which the particles highly need the diversification.

Here, the Self-Organizing Map (SOM) neural network is utilized to help to perform the *Gbest*computation mechanism. The SOM consists of an input layer and an output layer called Kohonen's layer. The output layer can be one- or two-dimensional. Read more about SOM in [11]. The SOM algorithm is described as follows. The input vector or input pattern presented to SOM for denoting its corresponding class/cluster can be defined by:

$$X = [x_1, x_2, \dots, x_D]^T \tag{6}$$

where*D* is the maximum number of features considered for each input pattern *X*. The weight vectors of the neurons in the output layer can be considered as:

$$W_i = [w_{1i}, w_{2i}, \dots, w_{Di}]^T; i = 1, 2, \dots, M \tag{7}$$

where W_i is the weight vector of the neuron *i* in the output layer which is representing a cluster, *D* is the total number of dimensions of the neurons' weight vectors and *M* is the number of neurons/clusters. Similar to any other type of neural networks, the SOM must be first trained to be prepared for clustering data sets/patterns. In the training process, all input patterns (here, the *Pbest* particles determined at each iteration) are inserted into the SOM network one-by-one. Once an input pattern is presented to the SOM, a competition is started between all SOM's neurons. The Euclidean distance between each neuron's weight vector and the input vector is calculated and the neuron that minimizes this Euclidean distance is identified to be the center of the corresponding cluster of the input vector and wins the competition. The winning neuron, then, moves toward the imposed input vector (*Pbest* particle) based on the Eq. (8):

$$W_i(t+1) = W_i(t) + \eta(t)(X - W_i(t)) \tag{8}$$

where$W_i(t)$ is the i^{th} neuron's weight vector in the iteration *t* and $W_i(t+1)$ is the weight vector of i^{th} neuron at the iteration *t* + 1. $\eta(t)$is the variable learning-rate parameter. One can define $\eta(t)$to monotonically decrease when *t* increases, as follows:

$$\eta(t) = \eta(0)\exp(\frac{-t}{\tau_1}) \tag{9}$$

where$\eta(0)$ is set to 0.1 and τ_1 is set to the maximum number of SOM iterations [12]. In this paper, τ_1 is set to be four times the number of the input vectors (*Pbest* particles). Thus, the SOM divides the *Pbest*particles into a variable adaptive number of clusters calculated by the Eq. (10):

$$N_{cluster}(t) = Round(N_{cluster}(1) - \frac{[N_{cluster}(1) - N_{cluster}(t_{max})]}{(t_{max}-1)} \times (t-1)) \tag{10}$$

where$N_{cluster}(t)$ is the number of clusters at the t^{th} iteration and t_{max} is the maximum number of iterations. In this paper, $N_{cluster}(1)$ is set to be the swarm size and $N_{cluster}(t_{max})$ is set to the value of 2 as the number of clusters at the final iteration. Then, the inverted number of the *Pbests* collected in each of the active clusters (the clusters having at least one *Pbest*) is obtained as the local diversity. The local diversity of each cluster can be taken as the weight of that cluster calculated as follows:

$$W_c^t = 1/|C_c^t|; for\ the\ clusters\ whose\ |C_c^t| \geq 1 \tag{11}$$

where W_c^t is the weight of the c^{th} active cluster at the t^{th} iteration and $|C_c^t|$ is the number of the *Pbest* particles collected in the c^{th} active cluster at the t^{th} iteration. Then, the best *Pbest* particle placed in each active cluster is designatedas the cluster best or*Cbest* particle. Finally, the unique *Gbest* particle for each particle can be calculated via a weighted averaging over all other (opposite) *Cbests*, i.e. all cluster centers excluding the

cluster center to which the focused particle's*Pbest* is belonging. The Eq. (12) depicts the way to calculate the *Gbest* for each particle.

$$Gbest_i^t = \frac{\sum_{\substack{j=1 \\ j\neq c(i)}}^{N_{cluster}(t)} W_j^t \times Cbest_j^t}{\sum_{\substack{j=1 \\ j\neq c(i)}}^{N_{cluster}(t)} W_j^t} \quad (12)$$

where $Gbest_i^t$ is the unique *Gbest* particle for the i^{th} particle at the t^{th} iteration, W_j^t is the weight calculated for the j^{th} cluster at the t^{th} iteration, $Cbest_j^t$ is the *Cbest* particle of the j^{th} cluster at the t^{th} iteration and $c(i)$ is the cluster to which the i^{th}*Pbest* particle is belonging. Thus, the Eq. (3) is changed to Eq. (13) in GuASPSO algorithm by replacing $Gbest^t$by $Gbest_i^t$. Other calculations, updating relations and parameter settings are just as the same of the original PSO algorithm.

$$V_i^{t+1} = \chi\,[V_i^t + \varphi_1(Pbest_i^t - X_i^t) + \varphi_2(Gbest_i^t - X_i^t)] \quad (13)$$

In GuASPSO, at the first iterations, the number of clusters is large, such that nearly all single *Pbest*s or the *Pbest*s located in the less-densely populated regions are gathered in separate clusters. As a result, the fitness values of the cluster best particles (*Cbests*) are endowed less influence factor to guide the particles in the search space and the diversity of the clusters is imparted more influence factor. Accordingly, in the early iterations, it is possible to find a *Cbest* conducting the particles, while it is lacking a suitable fitness value. By lapse of iterations, the number of active clusters is decreased and the low-fitness *Pbests* with high degree of similarity are aggregated in the common clusters. Thus, by determining the *Cbests* of the clusters, it is more probable that the designated *Cbests* have relatively more fitness values than those they had in the previous iterations. Consequently, the influence factor of the diversity is less stressed and the influence factor of the fitness is more stressed as the iterations go on. This process could assist the algorithm to hold a suitable balance between exploration, in which the diversity of the solutions is the major problem and the exploitation, in which the solutions attempt to converge to the optimal point of the promising regions found in the exploration process.

4. RESULTS AND DISCUSSION

The mathematical formulation of the optimization model is depicted below:

$$Minimize\ Z = \sum_{t=1}^{T}\left[\frac{De_t-(Re_t+Sp_t)}{De_t}\right]^2 + P_{s_1} + P_{s_2}\,; t = 1, 2\,, 3, \dots, T \quad (14)$$

$$S_t = S_t + Q_t - Re_t - Sp_t - Loss_t \quad (15)$$

$$Loss_t = EV_t - P_t \quad (16)$$

$$Re_{min} \le Re_t \le De_t \quad (17)$$

$$Sp_t = \begin{cases} S_t + Q_t - R_t - Loss_t - S_{max}; & if\ \ S_t + Q_t - R_t - Loss_t > S_{max} \\ 0; & if\ S_t + Q_t - R_t - Loss_t \le S_{max} \end{cases} \quad (18)$$

$$P_{s_1} = k_1 \times \sum_{t=1}^{T}[max(sgn(S_{dead} - S_t), 0) \times (S_{dead} - S_t)/S_{dead}] \quad (19)$$

$$P_{s_2} = k_2 \times \sum_{t=1}^{T}\left[\left(S_{opt} - S_t\right)/S_{max}\right]^2; for\ t = 12, 24, 36, 48, 60 \quad (20)$$

where De_t is the water demand in *t*th month of the planning period in MCM; Re_t is the water released in *t*th month in MCM and Sp_t is the spilled water from the reservoir in the *t*th month in MCM. $S_t$is the reservoir storage in the *t*th month in MCM; Q_t is the inflow to the reservoir in *t*th month in MCM; $Loss_t$ is the net water loss from the reservoir surface in MCM; $EV_t$and P_t are the evaporation from and precipitation to the reservoir in the *t*th month in MCM, respectively. $S_{max}$is the maximum volume of water the reservoir is designed to store, which is set to be 1470 MCM. $S_{dead}$is the dead water volume of the reservoir set to be 120 MCM. $S_{opt}$is the optimal storage volume set to be 400 MCM for the last month of each water year, to facilitate the reservoir operators to release the water to supply the agricultural water demands in each year. Furthermore, P_{s_1} and P_{s_2} are the penalty functions to mainly control the storage volume of the reservoir.

In the climate change scenarios studied in this paper, the parameters of precipitation and evaporation from the surface of the reservoir are all obtained from the data existing in each of the scenarios. The precipitation can be directly reached depending on which of the scenarios is focused, but the evaporation should be calculated based and in terms of the temperature as one of the important climatic change data existing for

each of the scenarios. In this paper, a non-linear regression relation is held between the temperature and the evaporation to achieve the evaporation. Furthermore, the volume of the precipitation and evaporation from the reservoir surface is assumed to be mainly dependent on the reservoir area which is dynamically varying during the planning period, while the height of the precipitation and evaporation (volume per unit area) are all considered to be constant disregarding the reservoir area. These heights are all already calculated via regression as depicted before. Furthermore, the inflow of the reservoir is estimated by HEC-HMS simulation model, based on the future climate change affected data. The water demands are all estimated regarding the correlation of the precipitation and the inflow occurring in each scenario with those observed in a long-historical period of the years. Finally, demands of the year the precipitation and inflow of which is the most correlated with those of each year in the future planning period, is adopted to be the water demands of that year. The planning period is a five-year near-future period, beginning from the water year 2018-2019 and ending to the water year 2022-2023.

In the first year of the planning period of the scenario B1, the water demands are at the least level contributing the demand percentage met to reach 62%, annually. However, the average reservoir storage is obtained to be 353 MCM, which might be considered to be the lowest over the five-year period, mainly due to the fact that in this year, the optimal reservoir operation is just starting. In the next year, the annual demand is twice of that in the first year, while the annual precipitation is half of that of the first year. Furthermore, the inflow is less than that in the first year by 29%, all of which contribute to meeting the water demands at the lowest level over the planning period equal to 28%. However, the average storage of the reservoir can be set to be 413 MCM, as a desirable storage for this dry year. The third and fourth water years are deemed to be the normal years, as regarding the climate change conditions, in which 51% and 57% of the water demands are averagely met. Moreover, the reservoir storage has exceeded the amount of 500 MCM, as the desirable water storage expected for a reservoir to have in an optimal reservoir operation, especially in the climate change conditions. These figures show the maximum potential of the Zayandehroud reservoir to handle the climate change to hold a balance between maximization of the portion of downstream water demands to be met and also the maximization of the sustainability of the reservoir. In the final year of the planning period, the inflow is declined by 25%, compared to the two previous years, contributing the demand percentage met to be reduced to 45% and the water to be stored in the reservoir at 440 MCM. These figures are all worse than those obtained in the third and fourth years of the planning period.

In the scenario A2, the average amount of the precipitation and the inflow have both decreased by 17% and 12%, as compared to those observed in the B1 scenario, illustrating the more acute climatic conditions in this scenario. At the first year of the planning period in the scenario A2, 49% of the demands are met, while the reservoir has stored only 249 MCM. In the second year, the reservoir is facing the same demands and the lower precipitation and inflow, while the storage can be raised to 339 MCM, which is more than the water stored in the first year. The main reason solving these conflict conditions is hidden in the fact that the initial year is coming from a streak of the dry years which in turn was making the reservoir vulnerable and hard to revive,while the second year is coming from the first year of the management period and thus, can be much more easily managed. In the third year of the period, the water demand percentage met is declined by 28%, mainly due to dramatic increase of the water demands by 64%. In the last two years, 67% of the demands are met and the storage is reaching nearly 450 MCM. The results obtained for these years, represent the best management policies applied to the reservoir by the optimization model, at least compared to three other years of the planning period of the scenario A2. Figure 2 illustrates the demands versus water supply resulting from the optimization.

In general, when operating the reservoir in the spring and summer, the low inflow is not only unable to recharge the reservoir and enhance the storage volume of the reservoir, but also does not suffice to supply the downstream demands without exploiting the reservoir storage. Thus, in a natural trend in operation, the storage decreases and is turned into the reservoir release, while the inflow is also fully dedicated to support the proper volume of the water released from the reservoir. Thus, the inflow along with a portion of the reservoir storage should participate to support the release of the reservoir and supply the downstream water demands. This is why the volume of the inflow is always less than that of the water released from the reservoir in the warm seasons of the year. In the autumn and winter seasons, the inflow to the reservoir increases, mainly as a result of the abundance of the precipitation turned into run-off, such that this increased inflow is both able to raise the reservoir stored water level and also support the water release to supply the downstream demands. Therefore, the volume of the inflow is much more than that of the water released during the reservoir operation in the cold seasons, unlike that in the warm seasons. The variations of the storage volume, release and inflow over the planning period are illustrated in the Figure3.

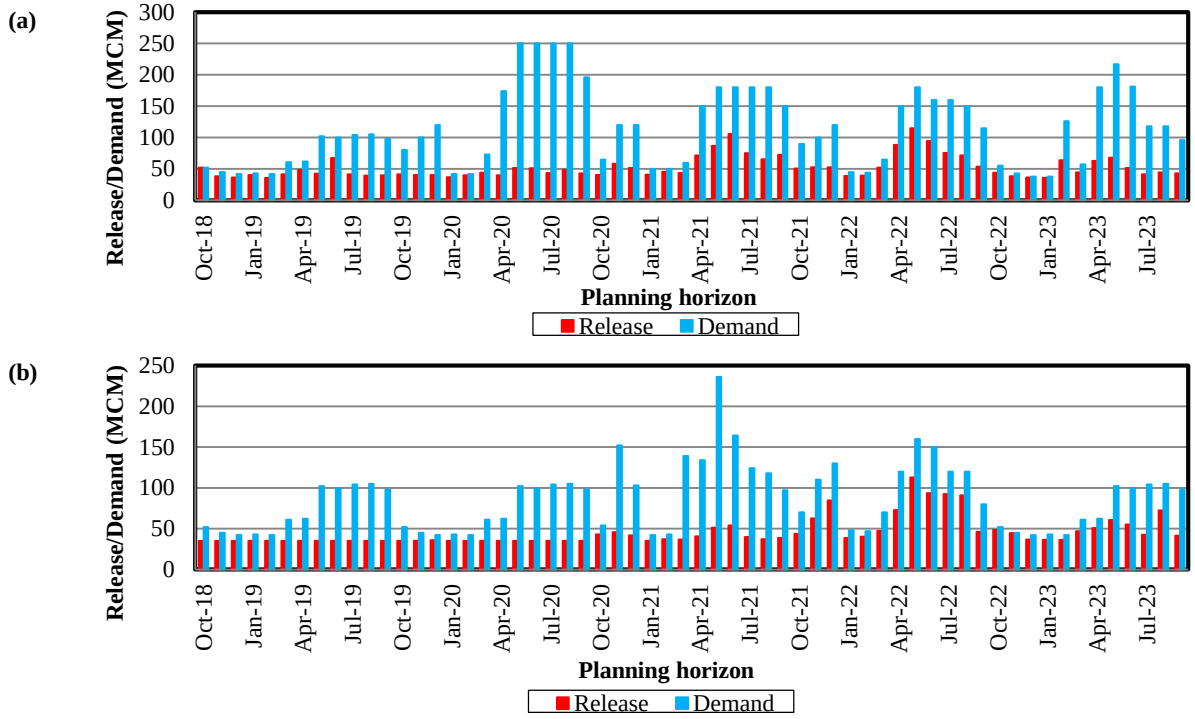

Figure2. Monthly water demands and the water released from the storage in the scenarios (a) B1; (b) A2

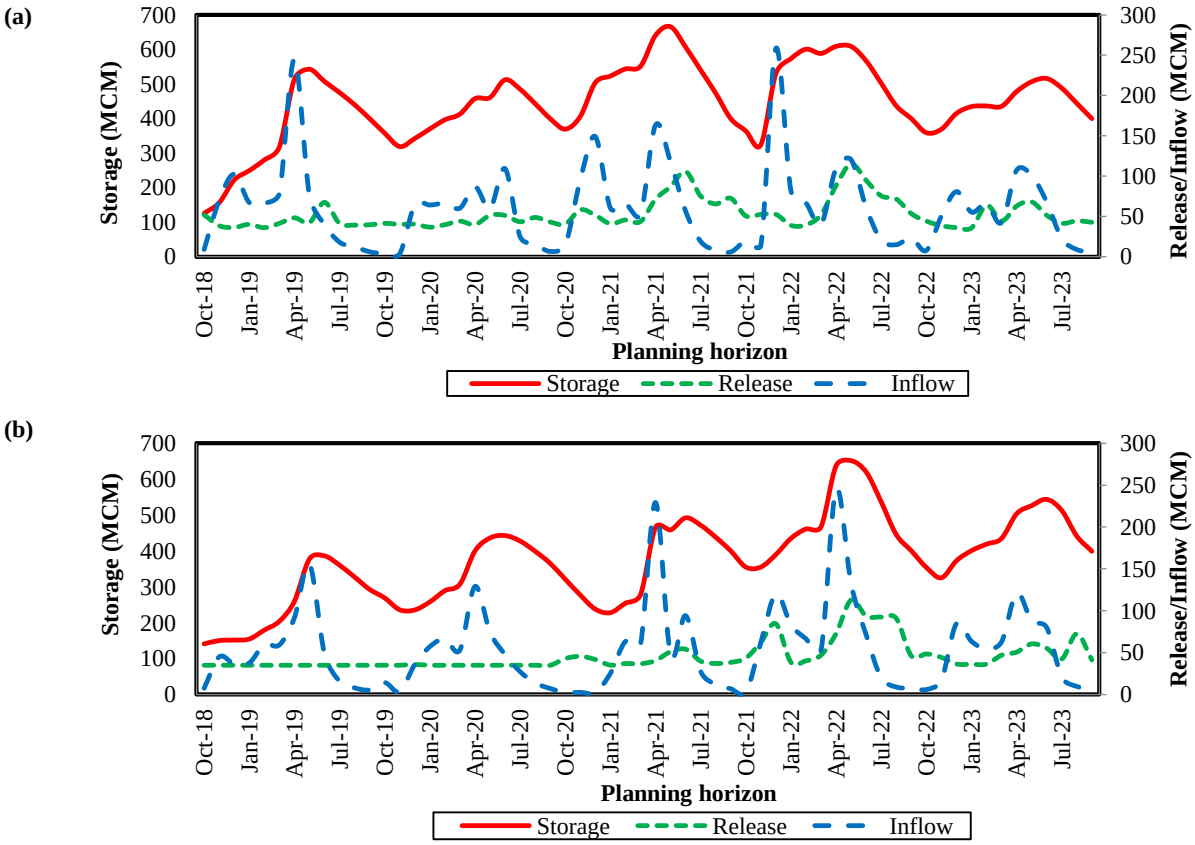

Figure3.Optimal storage, release and inflow over the planning period for the scenarios (a) B1; (b) A2

5. CONCLUSION

Due to human modifications of the landscape, many streamflow regimes throughout the world, including over one half of the world's large river systems, can no longer be considered natural. Primary human modifications include reservoirconstruction and irrigation projects, which, in some cases, canmask, dampen, or even change the sign of natural streamflowtrends.In the Fourth Annual Intergovernmental Panel Assessment Report, the four main scenarios of A1, B1, A2, and B2 (SRES scenarios) are modeled with five subcategories for each one. Among these scenarios, the scenarios A2 and B1 seem to be more realistic as compared to other ones, since the scenario A2 warns the human to face a rapidly growing population throughout the world and also a decreasing rate of the economic growth, and the scenario B1 mainly emphasizes the equal potential of the different communities to use the clean energies in order to mitigate the environmental effects of the climate change in a rapidly expanding world. This paper focuses on the simulation of the scenarios A2 and B1 to generate the hydrological data required to optimally operation of the Zayandehroud reservoir in the five near-future years under these climatic scenarios. A robust newly-proposed Guided Adaptive Search based Particle Swarm Optimization (GuASPSO) algorithm is utilized to solve the reservoir operation problem put forward in this paper. The GuASPSO is a new variant of the PSO algorithm, developed to hold an enhanced exploration-exploitation balance in the PSO algorithm. This algorithm can maintain the distances of the search particles with their global best guide particles in a moderate and well-balanced manner, such that the particles are neither to be trapped in local optima, nor engaged in a drift to compel the search space to lose diversity. Furthermore, an adaptive elitism mechanism is also predictedto be in the GuASPSO algorithm to further ameliorate the performance of the algorithm in diversification of the search space at the early iterations and intensification of the search at the last iterations of the optimization process. The results of the reservoir operation optimization suggest maintaining the average water storage of the reservoir over the five-year planning period at a desirable amount and also supplying the downstream water demands as much as possible. However, the management of the reservoir operation is more suitably carried out on the planning period under the B1 scenario, compared to the A2 scenario, as could be predicted from the nature of these scenarios and their special characteristics assumed for the water resources and demands, as well.

REFERENCES

1. Ficklin DL, Robeson SM, Knouft JH (2016) Impacts of recent climate change on trends in baseflow and stormflow in United States watersheds.Geophys ResLett 43:5079–5088.
2. Puff NL. (1997). The natural flow regime. Bioscience 47:769-784.
3. Abatzoglou JT, Barbero R, Wolf JW, Holden ZA (2014) Tracking interannual stream-flow variability with drought indices in the U.S. Pacific Northwest. J Hydrometeorol15:1900–1912.
4. Ficklin, DL, Abatzoglou, JT, Robeson SM, Null, SE AND Knouft JH. (2018) Natural and managed watersheds show similar responses to recent climate change. Earth, atmospheric,And planetary sciences journal.Vol 115.No 34. 8553-8557

5. Nilsson C, Reidy CA, Dynesius M, Revenga C (2005) Fragmentation and flow regulation

6. Lettenmaier DP, Wood EF, Wallis JR (1994) Hydro-climatological trends in the conti-nental United States, 1948–1988. J Clim 7:586–607.

7. Groisman PY, Knight RW, Karl TR (2001) Heavy precipitation and high streamflow in thecontiguous United States: Trends in the twentieth century. Bull Am MeteorolSoc 82:219–246.

8. Mohajeri, Sh, (2017) Integrated Water Resources Management Zayandehrud. Published by inter 3 institute for resource management GmbH.

9. Rezaei, F, Safavi, HR (2019) GuASPSO: a new approach to hold a better exploration-exploitation balance in PSO algorithm. Soft Computing, https://doi.org/10.1007/s00500-019-04240-8.

10. Kennedy, J, Eberhart R (1995) Particle swarm optimisation. 1995. In: Proceedings IEEE International Conference on Neural Networks, vol IV, pp 1942–1948. IEEE Service Center, Piscataway

11. Haykin, S(2009)Neural networks and learning machines, 3rd edn. Prentice Hall, Englewood Cliffs.
12. Chen, L–H., Chen, C–T., Lin, D–W. (2011) Application of integrated back-propagation network and self-organizing map for groundwater level forecasting. Journal of Water Resources Planning and Management, 137, pp. 352-365.